

# Chapter 5

## Comfort and Energy Implications of Urban Microclimate in High Latitudes



Maria Kolokotroni and Agnese Salvati

### Abbreviations

CFD	Computational fluid dynamics
DTM	Dynamic thermal modelling
EPBD	Energy Performance of Buildings Directive
<i>H/L</i>	Canyon aspect ratio
IPCC	Intergovernmental Panel on Climate Change
SUHI	Surface urban heat island
TRY	Typical reference year
UA	Urban albedo
UHI	Urban heat island

### 5.1 Introduction

The latitude of a location determines solar radiation received on horizontal and vertical building and urban surfaces; higher latitudes in both earth hemispheres receive less solar radiation than lower latitudes.

Figure 5.1 shows daily insolation for selected latitudes in the north hemisphere; higher latitudes receive most of the solar radiation during the summer months resulting in higher air temperatures in the summer compared with winter months. This results in seasonal variations in climatic conditions with winter months characterised by lower ambient temperatures compared to summer which in turn impact the energy demand by buildings to maintain thermal comfort.

In characterising the general climate of a location, geography studies typically use the Köppen-Geiger system. Figure 5.2 shows a world map of this classification. In simple terms, although latitude affects climatic conditions, the radiation energy

---

M. Kolokotroni (✉) · A. Salvati

Department of Mechanical and Aerospace Engineering, College of Engineering, Design and Physical Sciences, Brunel University London, London, UK

e-mail: [maria.kolokotroni@brunel.ac.uk](mailto:maria.kolokotroni@brunel.ac.uk)

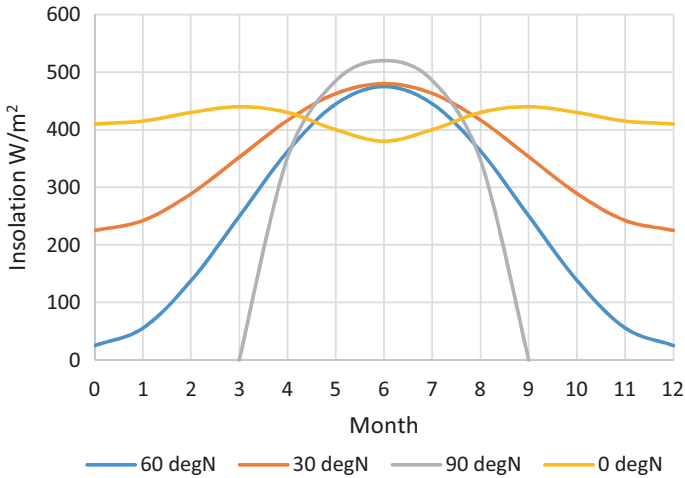


**Fig. 5.1** Daily insolation through the year at four latitudes in the north hemisphere. (Redrawn from <https://geography.name/insolation-over-the-globe/>)

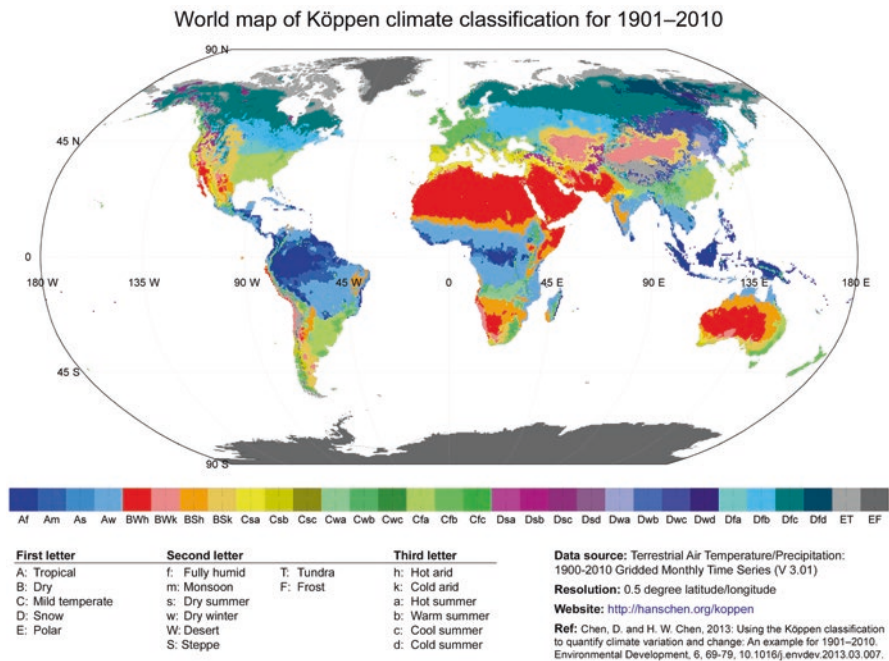


**Fig. 5.2** World map of Köppen climate classification, (modified from Chen and Weiteng 2013)

balance, tilt of earth, altitude, proximity to water and prevailing winds form the general climatic conditions. There are five different types of Köppen-Geiger climate classification: (A) tropical, (B) dry, (C) temperate, (D) continental and (E) polar (World Atlas 2020), following latitude but with variations.

Tropical zones receive intense solar radiation throughout the year and seasonal variations start to exist as we extend to the Tropics of Cancer and Capricorn ( $23.5^\circ$ ). These areas have two peaks of solar radiation during the year. The dry zones lie between the tropics and around  $35^\circ$  and have a strong seasonal cycle and a large annual insolation. The mild temperate and continental zones between latitude  $35^\circ$  and  $60^\circ$ , north and south, are characterised by seasonal contrasts in insolation and experience a large range in annual surface temperature. The zones above  $60^\circ$  have an extremely large yearly variation in day length, with enormous contrasts in insolation over the year with some months' insolation approaching zero.

Within the mild temperate zones (type C), two main subgroups of climates exist, depending on the latitude and the amount of precipitation and its distribution over the year. Lower latitudes, between  $35^\circ$  and  $45^\circ$ , are characterised by dry summers and are known as "Mediterranean climate" (Csa and Csb) while higher latitudes, between  $45^\circ$  and  $60^\circ$ , have higher precipitation and lack of a dry season (Cfb and Cfc). This chapter focusses on these high-latitude temperate regions, with higher heating requirements for buildings compared to cooling requirements.

Section 5.2 presents a description of the urban microclimate from global to local scale. Studies on surface and air UHI in high-latitude cities are described as well as the relationship between UHI and building energy demand in high-latitude cities. It continues with a description of microclimate impacts on ambient temperature using London as a case study of high-latitude location.

Section 5.3 focusses on urban albedo. Its definition is given together with the contributing parameters to its value. Available literature on the impact of these parameters on the urban albedo is presented. Results of a recent study of urban albedo in London are presented.

Section 5.4 focusses on modelling tools enabling the study of microclimate impact on indoor thermal conditions. The application of such tools to a case study in London is presented as an example. Section 5.5 summarises the chapter.

## 5.2 Urban Microclimate: From Global to Local Scale

The thermal balance of cities is affected by the increased absorption of solar radiation, corresponding increase of sensible heat released by urban structures, higher anthropogenic heat, reduced urban vegetation and higher emission of infrared radiation (Akbari and Kolokotsa 2016).

The urban heat island (UHI), although more pronounced in high-radiation/high-ambient-temperature cities, has been measured and quantified in cities of high latitudes characterised by warm/cold summers. Studies can be divided into those based on surface temperature data and those measuring air temperature within cities. The

first are useful in providing trends and mitigation measures at urban scales while the second can give insights into urban thermal comfort due to microclimatic variations and energy demand by urban buildings.

### ***5.2.1 Surface and Air UHI in High-Latitude Cities***

Peng et al. (2012) have reported on the surface UHI for 419 global big cities with population more than one million in 2007. The analysis was based on land surface temperature and considered the parameters of vegetation, urban albedo, climate and several socio-economic indexes. They showed that the average annual daytime is higher than the annual night surface UHI across big cities while no correlation was found between daytime and night. The distribution of night surface UHI correlates positively with the difference in albedo and night lights between urban and suburban areas indicating the impact of materials used, urban geometry and anthropogenic heat. They note that city structure such as building density, height and surface materials could also affect the night surface energy exchange, thus impacting the night surface UHI. No obvious effect of city size was found although it is noted that other studies found larger urban heat island intensity in bigger cities in one country or region. They concluded that because the 419 big cities are from different countries, different climatic zones and different economic development, the effects of city size could be masked by these factors. The distribution of daytime surface UHI (SUHI) correlates negatively with the difference of vegetation cover and activity between urban and suburban areas. The heat island intensity also varies seasonally. Daytime SUHI intensity has larger summer-to-winter amplitude than night SUHI intensity in the temperate regions over the northern hemisphere, and there are remarkable latitudinal variations in daytime SUHI intensity. Mid- to high-latitude cities (e.g. Beijing, Vancouver) have larger seasonal amplitude of daytime SUHI intensity than their low-latitude cities of similar size; for example, tropical cities where vegetation is active all year round show a flat seasonal profile of daytime SUHI intensity throughout the year. The evaporative cooling effects of the vegetation during the growing season may partly explain why the seasonal amplitude of heat islands differs between cities. The night SUHI intensity exhibits a small summer-to-winter amplitude of less than 1 °C for more than 86% of the big cities. The seasonal amplitude of night SUHI intensity is also more pronounced in cold regions (high latitudes) compared to warm regions (low latitudes). However, the seasonal amplitude of night SUHI intensity negatively correlates with both the mean temperature for the months when air temperature exceeds 0 °C and mean annual temperature. This result is consistent with the larger solar radiation energy transformed into SUHI intensity in summer over high-latitude regions. They note that the large SUHI intensity in summer not only increases the cooling power consumption in urban areas but also could increase the risk of heatwave extreme events over urban areas, as urban areas are affected by both global and local climate forcing.

The impact of latitude and climate on surface UHI was also reported by Zhou et al. (2014) for 32 cities in China. Results show that the SUHI differed substantially between day and night, with distinct climate-driven patterns, characterised by a higher SUHI in the south-eastern parts of China in the day and in the northern regions at night compared with other regions. In particular, the Northeast, with humid-cold climate, experienced the most intense SUHI across China. In addition, the SUHI intensity varied greatly with season, indicated by a relatively higher intensity in the day for the summer and at night for the winter across most cities. As a result, whether the daytime SUHI intensity was higher or lower than the night SUHI intensity depends strongly on the climate region and time period investigated. Overall, climate showed ultimate control on the SUHI spatial variability. In this study too the SUHI distribution in the day correlated significantly to vegetation activity and anthropogenic heat emissions in summer and to climate in winter, and at night was related closely to surface albedo, anthropogenic heat emissions, built-up intensity and climate in both seasons.

In studies of air temperature in urban areas, wind patterns are shown to have an impact. In Europe, UHI studies until 2007 are reported by Santamouris (2007); they are divided into the Mediterranean zone (Csa), central Europe and the UK (Cfb) and northern Europe (Dfc) as shown in Fig. 5.2. It was concluded that in cities in central Europe, the UK and northern Europe, maximum UHI values developed at night and similarly with Mediterranean cities do not show any relation to the city size. Greatest intensity was found in windless and cloudless conditions mostly in the summer similarly to Csa regions. Additional data for Europe are included in the work of Santamouris (2016).

At continental level Santamouris (2015) reported on UHI in Australian and Asian cities. Most cities reported are located in hot climatic zones but a few are cold/warm summer regions. The conclusions of this review introduce the impact of climatic conditions and wind on the formation of UHI which is not apparent in SUHI studies. The review concluded that the size of city correlates with magnitude but the method of data acquisition is important to quantify this. There is a seasonal variability as observed in SUHI studies; humid locations have the max UHI during dry periods rather than during warm periods. UHI is more pronounced at night consistent with SUHI studies but in some cities with hot climate and high density maximum UHI can be present during the day mainly due to anthropogenic heat. Also, cool islands have been observed due to shading, reduced anthropogenic heat and possible cooling effect of sea breeze. Calm and clear sky conditions help in the development of UHI but high wind speed can dramatically reduce it although wind speed thresholds to reduce UHI vary according to geometry and density while coastal cities mostly benefit from sea breeze.

The results reported at global level are more or less replicated in locations of high latitudes with cold/warm summers. An example is London. Figure 5.3 shows the UHI measured using fixed stations (Watkins et al. 2002a). The average annual UHI is 2.5 °C at night but there is wide variation including cool islands mainly during the day. Figure 5.4 shows the impact of solar irradiance which is mainly observed during days with meteorological wind speed more than 5 m/s (Kolokotroni and

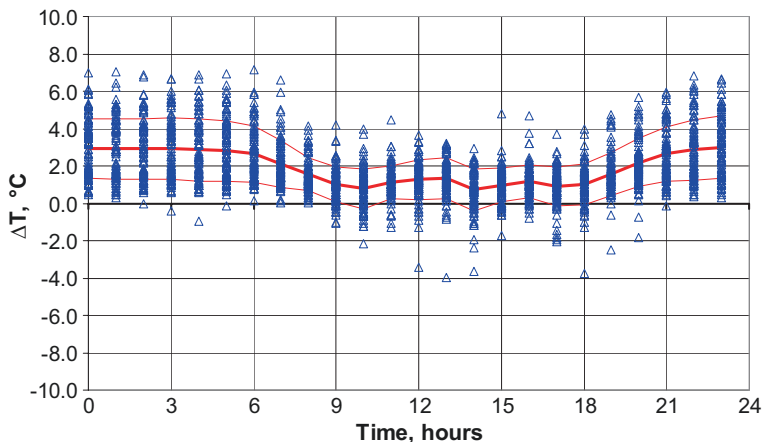


**Fig. 5.3** Hourly air temperature difference over 24 h between urban and reference locations in London measured at fix stations (source: Watkins et al. 2002a)

Giridharan 2008) while Fig. 5.5 shows that night UHI is independent of daytime air temperature during the summer; during the night similar difference between urban and rural air temperature was measured during a typical and hot week (Kolokotroni et al. 2006).

### 5.2.2 *UHI and Building Energy Demand in High-Latitude Cities*

At global level Santamouris (2020) reported on recent progress of urban overheating and urban heat island. Air temperature experimental results from 400 cities show that the magnitude of the average temperature increase may exceed 4–5 °C while at the peak may exceed 10 °C. The paper reviews UHI impact on energy demand by buildings and impacts on outdoor air quality and health. In terms of energy demand, the analysis shows that the total increase in energy demand is close to 12% considering all locations and building types and the actual magnitude is strongly correlated with the magnitude of UHI. In most cases the reduction in heating energy demand is less than the increase in cooling energy demand resulting in a net increase. This net increase depends on ambient temperatures during the cooling season but is also related to building type and its energy efficiency strategies.

For locations with warm/cold summer conditions, low cooling demand for well-designed buildings should result in low increase in cooling demand despite the UHI; however cooling demand has increased during the last years in these locations too. There are two reasons for this: first increasing ambient temperatures due to climate change combined with the UHI, and second regulations for energy efficiency focused on winter conditions with the unintended consequence of overheating

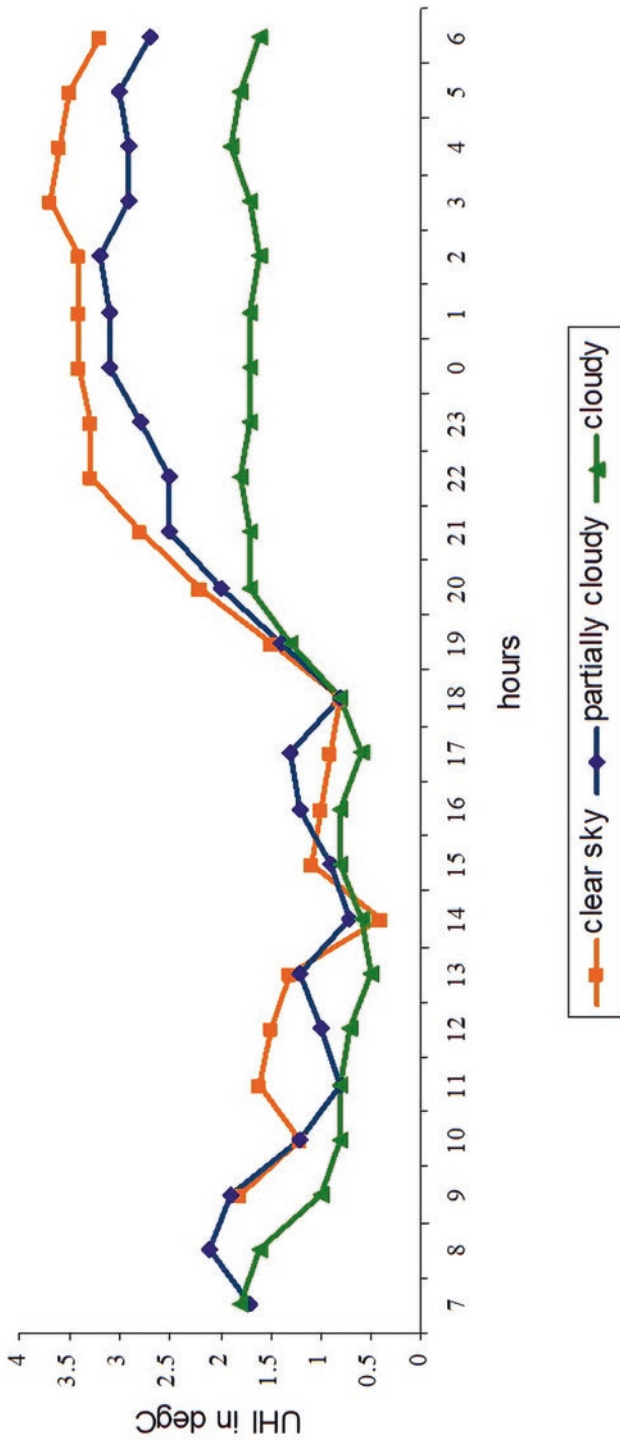


**Fig. 5.4** Effect of solar irradiance on hourly air temperature difference over 24 h between urban and reference locations in London at fixed stations (adapted from Kolokotroni and Girdharan 2008)

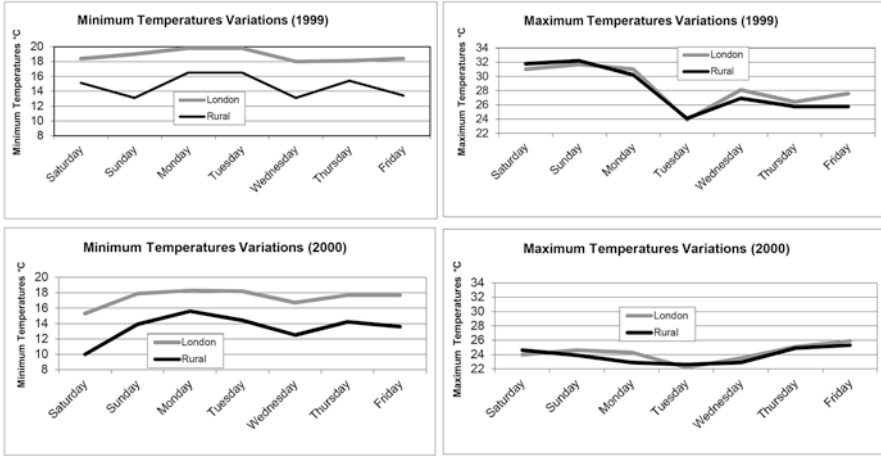


Fig. 5.5 Minimum and maximum air temperature in London and reference site during a typical and hot week (adapted from Kolokotroni et al. 2006)



Fig. 5.6 A transect through London showing air temperature fixed stations from West to East (Kolokotroni et al. 2012)

during the summer season. In buildings without cooling, overheating is also a consequence which impacts comfort and health.

This impact on energy demand and overheating has been studied in detail for office buildings in London (Kolokotroni et al. 2012). Figure 5.6 shows a transect through London (West to East) where air temperature was measured at fixed stations (Watkins et al. 2002a). The model of a typical office building was created and thermally simulated using the city’s Test Reference Year (TRY) weather file from



the Heathrow Airport weather station and urban TRY files in which air temperature was changed to correspond with hourly measurements at each transect point. Figure 5.7 shows the increase in overheating hours in the free-floating office across the transect compared to the rural position. It also shows the impact of future climate change by presenting simulation results using the 2050 future weather file. This was created by first modifying the Heathrow TRY weather file using the climate projections of the Intergovernmental Panel on Climate Change (IPCC) for medium-high emission scenario. The air temperature was then changed to superimpose the measured air temperature in each of the transect locations assuming that the UHI will be the same in the future. Figure 5.8 shows the interurban and future variation of cooling energy demand assuming for an air-conditioned office with a cooling setpoint temperature of 24 °C.

The impact of UHI and climate change on energy demand is as expected and in the magnitude reported in literature (Santamouris 2016) for heating-dominated climates. What is interesting for building designers is the impact of energy efficiency measures and their performance in the future. Figure 5.8 shows that at present, offices with medium internal heat gains without night free cooling have similar cooling demand to offices with high heat gains and night free cooling. In the future, and because of higher night temperature due to the combined effect of climate change and UHI, offices with medium internal heat gains perform better than those with night free cooling.

Figure 5.9 shows that as expected heating demand is lower in offices within the UHI and even lower in the future. Night cooling is not shown as it is not used during the heating season.

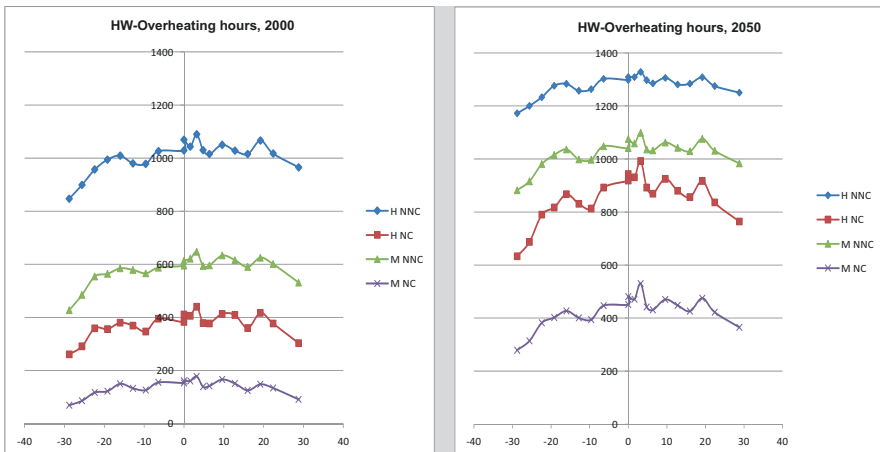


**Fig. 5.7** Predicted overheating hours (>28 °C) during occupancy hours using modified weather files for urban location and climate change for a typical office in 20 locations on the West-East axis of London (*HW* heavy weight construction, *H* high heat gains, *M* medium heat gains, *NC* night cooling, *NNC* no night cooling) (Kolokotroni et al. 2012)

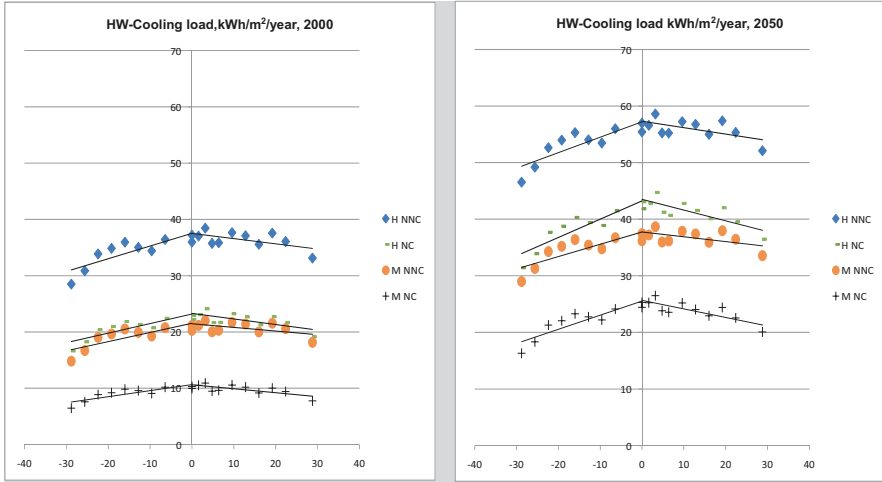


**Fig. 5.8** Predicted normalised annual cooling load using modified weather files for urban location and climate change for a typical office in 20 locations on the West-East axis of London (*HW* heavy weight construction, *H* high heat gains, *M* medium heat gains, *NC* night cooling, *NNC* no night cooling) (Kolokotroni et al. 2012)

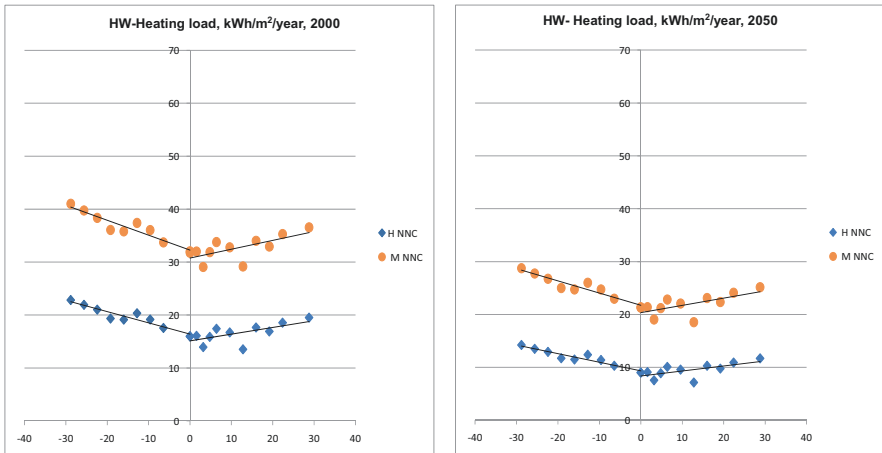


**Fig. 5.9** Predicted normalised annual heating load using modified weather files for urban location and climate change for a typical office in 20 locations on the West-East axis of London (*HW* heavy weight construction, *H* high heat gains, *M* medium heat gains, *NNC* no night cooling) (Kolokotroni et al. 2012)

Therefore, in terms of energy demand by buildings, in high-latitude cities with warm/cold summers where most buildings are not air-conditioned, UHI helps reduce the building energy consumption, at present. However, building will be

air-conditioned in the future because of higher temperatures and even higher in the city.

Once air conditioning is introduced, internal temperatures will be regulated at the range of 21–24 °C. At present, we tolerate higher. Estimations indicate a five-fold increase in carbon emissions by city buildings in 2050 (Kolokotroni et al. 2012).

There are various strategies to mitigate this; these include the following:

- (a) Improve energy efficiency and passive cooling design of buildings in high-latitude cities, to avoid overheating risk due to urban and climate change effects. This is already regulated in many regions for example through the Energy Performance of Buildings Directive (EPBD) in Europe.
- (b) Generate heat and electricity by building integrated renewables—nearly zero-carbon buildings—this is coupled to (a) and again regulated in many regions.
- (c) Improve external thermal environment; this is not regulated yet but initiatives and studies indicate its importance. Mitigation strategies include the following:
  - Reduce anthropogenic heat from buildings and transport; this is related to improved energy efficiency in buildings and use of passive strategies where possible to reduce rejected heat from cooling systems. Transport is also regulated mainly due to interventions to reduce vehicle emissions with electric vehicles increasing in many cities.
  - Increase vegetation.
  - Increase albedo of surfaces.

The following section attempts to answer the question of ‘what is the impact of vegetation and surface albedo in the microclimatic scale in high latitudes?’ taking London as a case study.

### ***5.2.3 Microclimate Impacts on Ambient Temperature: London Case Study***

The impact of vegetation (parks and green spaces) on the ambient air temperatures has been studied in London. Figure 5.10 shows measurements inside and outside a park over 1 day (Watkins et al. 2002b). Air temperatures are lower inside the park. There is more pronounced variation outside indicating the impact of other microclimatic variables such as canyon geometry and prevailing wind. Figure 5.11 shows the air temperature difference between the park and outside during the daytime. Air temperature is lower in the park consistent with findings of the effect of vegetation at the scale of the city (Peng et al. 2012).

A study on the impact of small areas of vegetation was carried out in a suburban area of London during day and night-time (Maciel et al. 2013). Figure 5.12 shows that air temperature in green locations is lower during the night with the difference increasing as ambient temperature increases.

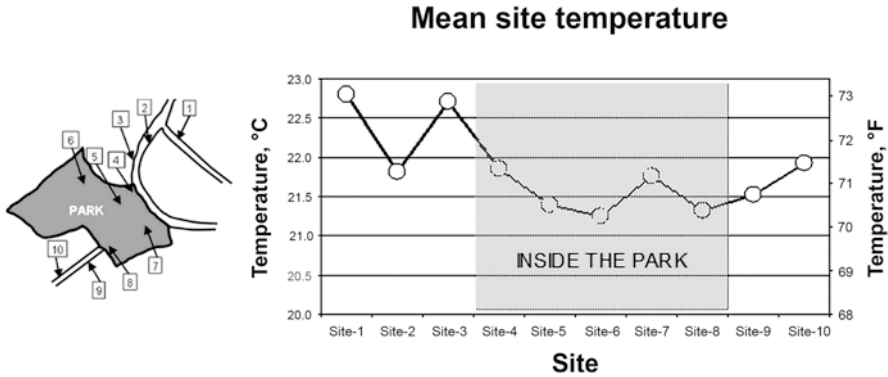


Fig. 5.10 Mean site air temperature over 1 day, showing the effect of vegetation (Watkins et al. 2002b)

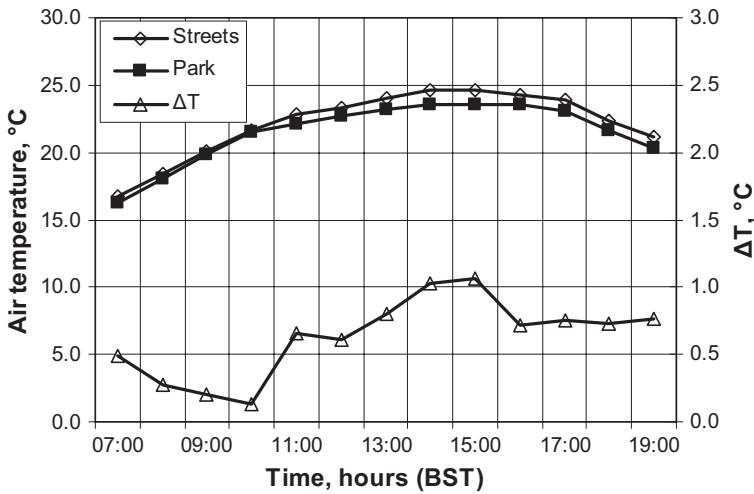
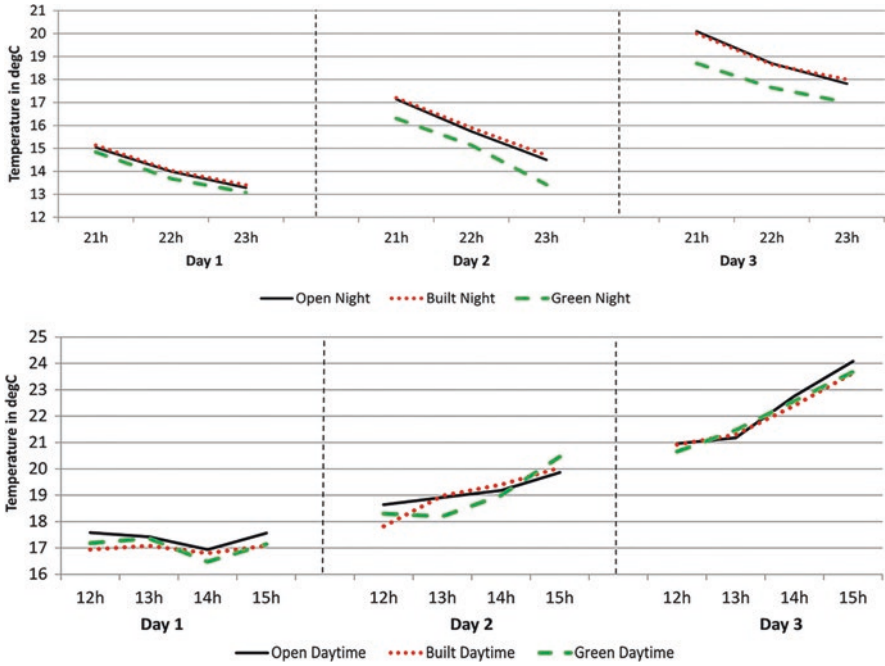


Fig. 5.11 Air temperature inside and outside the park over the day, indicating maximum difference during early afternoon (Watkins et al. 2002b)

The impact of roof reflectivity was measured on a building at the same site (Kolokotroni et al. 2013). Figure 5.13 shows the reduction of roof surface temperature with changed albedo from 0.1 to 0.6 (in situ measurements).

Road and pavement with high albedo can change the air temperature above these surfaces. This has been studied extensively as a method to mitigate UHI and increase external thermal comfort (Akbari and Kolokotsa 2016). In addition it can help to extend the effectiveness of passive cooling strategies such as natural ventilation (Maciel and Kolokotroni 2017) as shown diagrammatically in Fig. 5.14. Cool surface temperature could be 20–30 K less than asphalt and measurements have shown a 10 K air temperature difference at 75 cm above the surface.



**Fig. 5.12** Air temperature measured during day and night at locations with open aspect (mainly roads), built aspect (next to buildings) and green aspect (mainly grass) (Maciel et al. 2013)

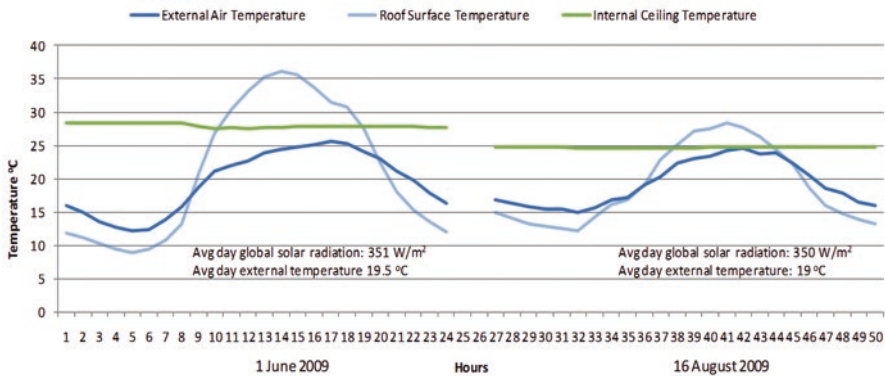


**Fig. 5.13** Measured air and surface temperature of the case study building on 2 days, one in June (pre-paint period) and the other in August (after-paint period) during which external temperature and solar radiation are similar (Kolokotroni et al. 2013)

The effect of building facade albedo was studied in central London (Watkins et al. 2002b). Figure 5.15 shows the results of these measurements; it can be seen that dark-coloured facades result in higher surface temperatures but overshadowing effects were clear. The figure also shows that facade surface temperatures impact the

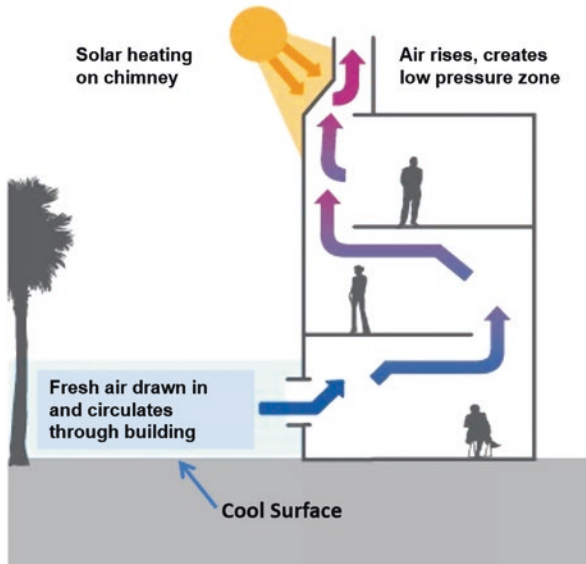


**Fig. 5.14** Diagram showing how cool pavements can enhance passive ventilation due to the enhanced temperature difference (Maciel and Kolokotroni 2017)

canyon air temperature while climatic conditions and solar radiation intensity determine the magnitude. These relationships are explained in more detail in Sect. 5.3 where the urban albedo is discussed.

### 5.3 Urban Albedo

Surface albedo is defined as the proportion of reflected short-wave radiation to the total incoming short-wave radiation upon a surface. The higher the albedo, the higher the reflected radiation and the lower the surface temperature, contributing to reduced heat island effects in urban areas. However, in an urban setting, the incoming radiation undergoes multiple reflections as it bounces between buildings. Therefore, ‘urban albedo’ is defined as the weighted mean value of albedo in a cluster of buildings, depending on both materials and urban geometry. Urban albedo is a major contributor to changes in outdoor surface and air temperature as discussed in Sect. 5.2.1, intensifying the urban heat island phenomenon which in turn impacts the outside thermal comfort and energy demand by urban buildings.

The factors that contribute to the value of urban albedo can be grouped into the following interrelated parameters:

- *Geometry*—the geometry of individual buildings, the building group geometry and the geometry of buildings in relation to roads, usually referred to as urban canyon geometry

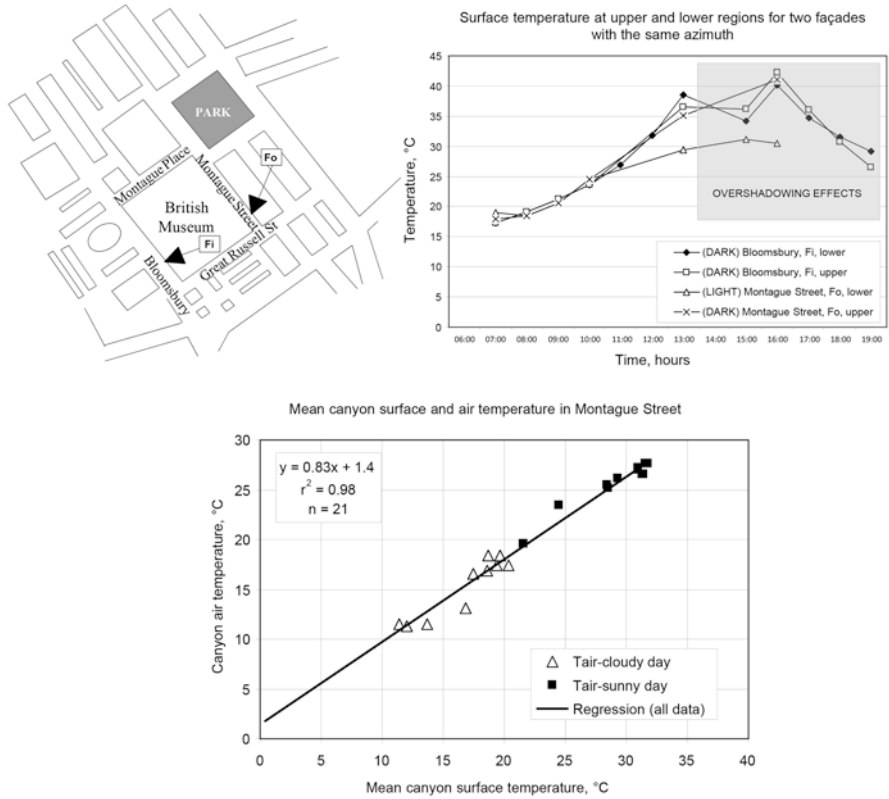


Fig. 5.15 Measured air and surface temperatures in two street canyons in central London (Watkins et al. 2002b)

- *Reflectance* of surfaces and their orientation—ground, facades and roofs

These two parameters are not related to latitude and climate, although climate impacts the urban development and materials used for buildings and there are indications that wetness of surfaces might affect reflectance.

- *Sun altitude and azimuth* determining the incidence angle of incoming solar radiation with strong seasonal contrasts in high latitudes

Geometry, surface reflectance and sun’s position are in many cases used to calculate the urban albedo.

- *Moisture* of permeable surfaces (soil) and altering reflectivity of impermeable surfaces
- *Vegetation* acting as obstruction to the incoming radiation and reflection paths

These three parameters are closely related to climate. Moisture is connected to climatic conditions (air relative humidity) and precipitation. Similarly, vegetation

types differ according to prevailing climatic conditions and in many cases are related to latitude (e.g. deciduous trees).

Models have been developed to predict urban albedo mainly based on computational analysis with the aim to predict the impact on energy demand by buildings; energy demand is further discussed in Sect. 5.4. Xu et al. (2020) developed a model to examine pavement albedo on energy impact in buildings in Boston. Salvati et al. (2020) proposed a methodology to consider urban form and climate impact on the energy demand by buildings. In both studies the following parameters are integrated in the models and include computation of the incidence angle of incoming solar radiation:

Building height ( $H$ ) and footprint area, street width ( $W$ ) and length of street ( $L$ ) define:

- The canyon aspect ratio ( $H/W$ ) which affects the amount of solar radiation incident on the canyon surfaces, as higher buildings and narrower canyons result in more shading and less incident radiation. This in turn can be computed as *building density* or site coverage ratio or plan area index which is the ratio of the buildings' footprint area to the urban site area.
- The ratio of the vertical surface area defines the *facade density* which is usually defined as  $H \times P$  (with  $P$  the perimeter of buildings) to the building footprint area. This ratio directly determines the area of buildings and building walls affected by changes in the amount of incident radiation received and reflected.

The impact of these parameters on the urban albedo was studied computationally by Yang and Li (2015) for Hong Kong. The study gives a concise literature review of urban albedo studies until 2015 both computational and experimental. The study reports seasonal variations of urban albedo with low-rise medium density (0.44) having the greatest ability to absorb solar radiation. Figure 5.16 (for  $H/L$  ratio of 1) shows that as density increases or decreases, it plays a dominant role in the radiation reflection process leading to an increase in urban albedo. Urban albedo is minimum for building density of about 0.45; for lower densities, urban albedo is higher because the higher distance between buildings eases the ability of urban texture to

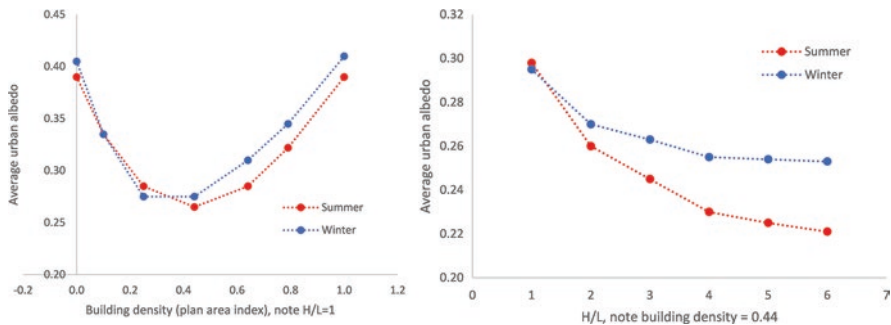


**Fig. 5.16** Urban albedo relationship with season, building density (plan area) and canyon aspect ratio  $H/L$  (redrawn from Yang and Li 2015)



reflect solar radiation toward the sky. Urban albedo is higher for building density above 0.44 due to the increased contribution of roofs to reflecting radiation out of the urban fabric. Urban albedo was found to decrease with increasing building height for a fixed building density.

It should be noted that the same geometrical parameters influence wind patterns in the canyon. Although wind effects have no impact on urban albedo, they influence surface and air temperature in the canyon (Yang and Li 2015; Salvati et al. 2020).

The daily variation of the urban albedo was reported by Qin (2015) studied computationally with experimental validation of measurements at the latitude of  $\sim 51$  in Poland for different canyon orientations and seasons (Pawlak and Fortuniak 2003). The parametric analysis carried out concluded that the canyon aspect ratio ( $H/L$ ) dominates the urban albedo while other parameters play a secondary role.

Recently, the urban albedo has been studied in London as a case study of high latitude (Urban Albedo 2019). A typical residential area was identified based on the work of Kolokotroni and Giridharan (2008) and is being studied with the aim to identify how the urban albedo can be estimated. Methods include the construction of a 1:10 model of the urban area where extensive measurements are carried out, selective measurements in the actual case study area, CFD modelling using ENVI-met calibrated by the physical and scale model measurements, ray modelling using Radiance and laboratory characterisation of the surface materials of the urban case study.



**Fig. 5.17** 1:10 scale model constructed at the University of Kent and full-scale spot measurements at the case study area in London

Figure 5.17 shows photos of the scale model constructed at the University of Kent, UK, and full-scale measurements taken at the case study area. The scale model represents a real residential area in London as indicated in Fig. 5.18.

*Results to date from the scale model* indicate that consistently with previous studies, the observed albedo peaks occurred at lower sun angles during morning and late afternoon hours in summer months. Therefore, within the same geometry, albedo was measured to peak at low irradiance ( $50\text{--}150\text{ W/m}^2$ ). As expected increase of paving reflectivity and wall reflectivity increased the urban albedo for the same geometry. This was observed mainly in dry conditions for radiation intensity up to  $350\text{ W/m}^2$  with marginal increase at higher irradiances. The observed increase of albedo due to the application of paving and facade colour disappears in rainy days, thus highlighting the dynamic nature of albedo. This is a significant observation for climates with frequent rainfall such as in London (Nikolopoulou et al. 2020).

*Results from field spot measurements* in the three urban canyons (as shown in Fig. 5.18) indicate no change in the urban albedo for different heights as shown in



**Fig. 5.18** Residential area in London where measurements were carried out and the 1:10 scale model is based on. Study by Salvati and Kolokotroni (2020a), aerial views from Google Earth

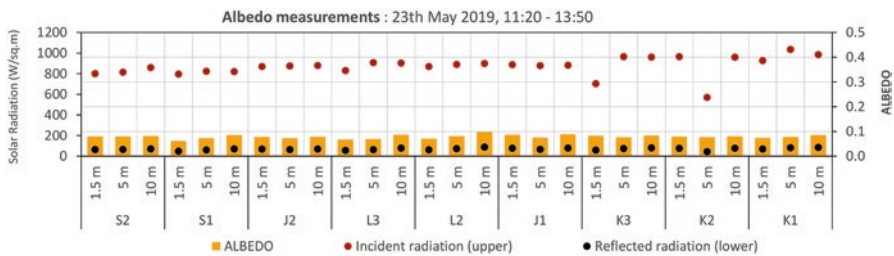


**Fig. 5.19** Measured incoming (incident) and outgoing (reflected) radiation and urban albedo values within urban canyons in the case study area (Salvati and Kolokotroni 2020a)

Fig. 5.19 (Salvati and Kolokotroni 2020a). The three canyons have the same  $H/W$  ratio of approximately 0.75 but different orientation and material distribution. The radiation measurements showed that, for a datum geometry, the reflections are not influenced by street orientation and material distribution. Also, the measured reflections did not vary with measurement height, being approximately the same value at the street level (1.2 m height), second-floor height (5 m) and eaves level (10 m). Therefore, the measured urban albedo, namely the ratio of the measured outgoing to the incoming radiation, showed very small variation. This can be explained by the dominant role played by the canyon geometry in trapping solar radiation and the low albedo of the road material (asphalt) in comparison to the albedo and the orientation of the facades.

ENVI-met was calibrated using the scale model and field measurements (Salvati and Kolokotroni 2019) and was used to study the impact of urban albedo changes on microclimate and outdoor thermal comfort. These results were first reported by Salvati and Kolokotroni (2020a, b). The canyon aspect ratio in the case study area is approximately 0.75 (building height equal to 12 m and street width equal to 16 m). In this kind of geometry, at London’s latitude, the simulation results show that increasing the wall albedo does not improve the outdoor thermal comfort while increasing the road albedo has a significant positive impact on the physiological equivalent temperature (PET) at the street level which is used for assessing outdoor thermal comfort (Hoppe 1999). This result is explained by the impact of the roads’ and facades’ albedo change on the air temperature and mean radiant temperature at street level, as reported in Fig. 5.20. The trends reported in the figure correspond to point S2 (see Fig. 5.18), but they are similar in all the canyons. In terms of air temperature, changing the albedo of facades does not influence air temperature. A

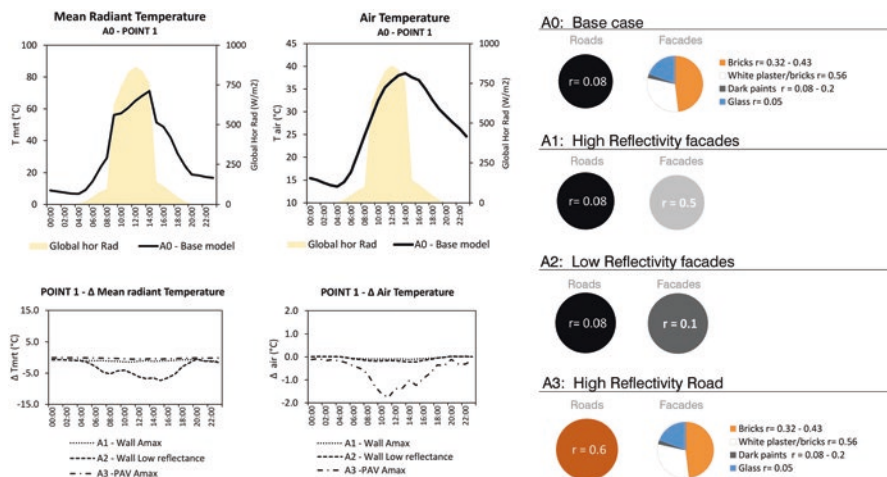


Fig. 5.20 Impact of roads and facades’ material reflectivity on air temperature and mean radiant temperature at street level compared to the current scenario (base case) (source: Salvati and Kolokotroni 2020a)

significant decrease of air temperature is instead obtained with the increase in road albedo (scenario A3). On the other hand, for the studied geometry, increasing the reflectivity of facades (scenario A1) has a negligible impact also on the mean radiant temperature. Conversely, a substantial decrease in facade albedo (scenario A2) allows a reduction of the mean radiant temperature at the street level.

Similar results were also reported in other latitudes (Alchapar and Correa 2016; Erell et al. 2014) and can be explained by the impact of the walls’ albedo on the multiple reflection of solar radiation within urban canyons. Similar results were found by Levinson (2019), who showed that the wall’s solar availability in an urban context may increase up to 30% in deep urban canyons when the albedo of the neighbouring building is raised from 0.25 to 0.6.

The impact of canyon aspect ratio ( $H/W$ ) and changes of reflective materials on UA was studied. The results are shown in Fig. 5.21 (Salvati and Kolokotroni 2020b). The reflective materials have a larger impact on low-rise aspect ratio canyons compared to high-rise ones. This is particularly evident for the scenario A2—reflective roads—which determines a much higher relative increase of UA in the canyons with aspect ratio of 0.75 compared to the ones with aspect ratio of 1.5. However, when the reflective materials are applied to the top half of the canyon’s facades (A1 TOP), the two canyon geometries show a similar relative and absolute variation of the UA.

This might be explained by the fact that the top half of the canyon facades receives a similar amount of solar radiation despite the different canyon geometry. The results presented in Fig. 5.21 indicate that the two canyon geometries have less variation of the UA for the base case materials compared to variations for other cases examined. However, this similarity does not result in the same microclimate at the street level, because the increase of building height determines a significant reduction of the solar radiation reaching the street level in the high-rise urban area. The results also indicate that the highest relative increase of UA is achieved with scenario A2 in the low-rise canyons and with the scenario A1 TOP in the high-rise canyons. Some differences exist in the UA of the three different canyons due to their orientation. Canyon 2 shows the highest variations of UA with the use of reflective materials since it is the canyon receiving the highest amount of solar radiation among the three analysed.

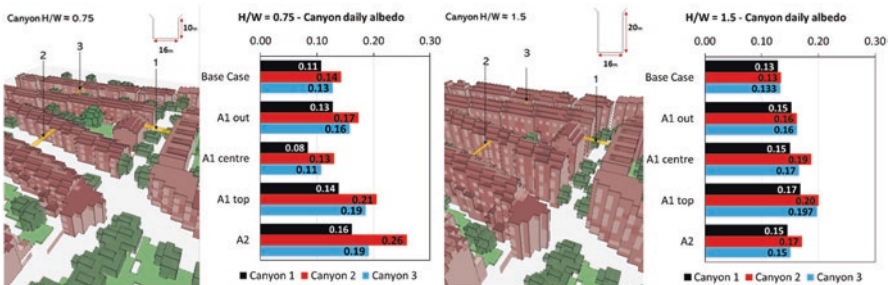


Fig. 5.21 Impact of the reflective material scenarios on the three canyons’ daily urban albedo (source: Salvati and Kolokotroni 2020b)

## 5.4 Modelling Tools: Impact of Microclimate on Indoor Thermal Conditions

Approaches have been proposed to include local climate in the energy performance simulations of buildings in urban contexts. However, in most proposed approaches, only a subset of the urban climate modifications are included in the analysis. A recent study carried out by the authors in collaboration with two other authors (Salvati et al. 2020) showed that in a dense urban context, building energy performance is significantly affected by urban air temperature but also by urban wind speed, solar access and surface temperature of surrounding buildings. The methodology proposed by Salvati et al. (2020) is based on the use of a suite of climate tools, including the *Urban Weather Generator* (Bueno et al. 2013; Mao et al. 2017), to calculate urban air and surface temperatures and empirical models to estimate wind speed in urban canyons. The calculation of the canyon wind speed was based on the URBVENT project approach (Ghiaus et al. 2004), applying different empirical models for different urban situations, depending on the geometry and orientation of the canyon and the wind speed and direction at the meteorological station. This modelling approach is suitable for building in dense urban areas, characterised by urban canyons with high height-to-width ratio. In less dense suburban areas, the impact of atmospheric and surface heat island is lower. However, the distribution of wind speed at the microscale may affect the thermal performance of naturally ventilated buildings also in suburban locations.

At the microscale, CFD microclimate models such as ENVI-met (Huttner and Bruse 2009) allow to simulate the spatial and temporal distribution of the airflow around buildings, considering the actual three-dimensional geometry of the building and its surroundings. A case study in London is presented as an example of the potential impact of the microscale airflow on the indoor thermal conditions of buildings.

### 5.4.1 Case Study

The case study is a student accommodation building located at the campus of Brunel University London (Fig. 5.22). This case study is part of the H2020 project ReCO2ST (2020) and was used to study the effect of microclimatic conditions on energy simulations. ENVI-met V4.4.4 was used to run simulations in full forcing mode, namely using local hourly values of air temperature, relative humidity, wind speed and direction as input inflow boundary to the three-dimensional CFD atmospheric model, increasing the model accuracy significantly. ENVI-met simulation outputs include the spatial and temporal distribution of wind speed and directions at the building facades. These were used as boundary conditions for dynamic thermal simulations of the building using EnergyPlus, to investigate their impact on the building air change per hour (ACH) and the indoor thermal conditions.

The microclimate simulations confirmed that the wind speed and direction at the building facades are significantly modified by the presence of the nearby trees and buildings, for any wind direction (Fig. 5.23). The staggered shape of the building also plays an important role, determining significant variation in the wind speed and pressure on facades with same orientation.

These form-driven effects on airflow and consequent wind pressure on facades are normally neglected in building performance simulation, unless for tall or special buildings. The normal approach for the calculation of wind pressure on facades is based on Bernoulli's equation, considering the wind pressure coefficients and the wind speed at the building height, by applying the power law profile to the meteorological wind speed. The main weaknesses of this procedure consist of (1) the simplified building forms for which pressure coefficients are available and (2) the calculation of the local wind speed based on the power law profile, which is not valid in the presence of large obstacles such as buildings and trees. The inaccuracy of the ventilation potential due to this approximation can be relevant, since the wind pressure calculation is proportional to the second power of the wind speed.

To assess the impact of the microclimatic wind speed conditions in comparison to the meteorological weather file, the ENVI-met outputs were used to calculate the

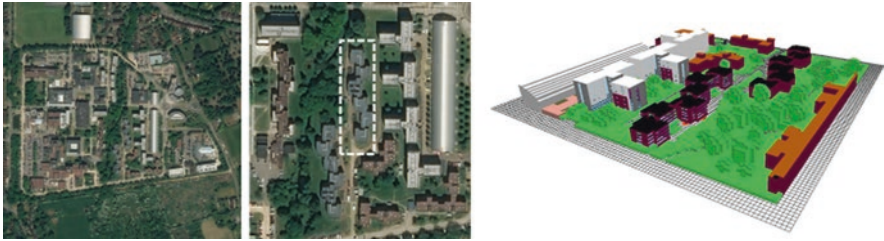


Fig. 5.22 Aerial view of the case study building and corresponding ENVI-met model

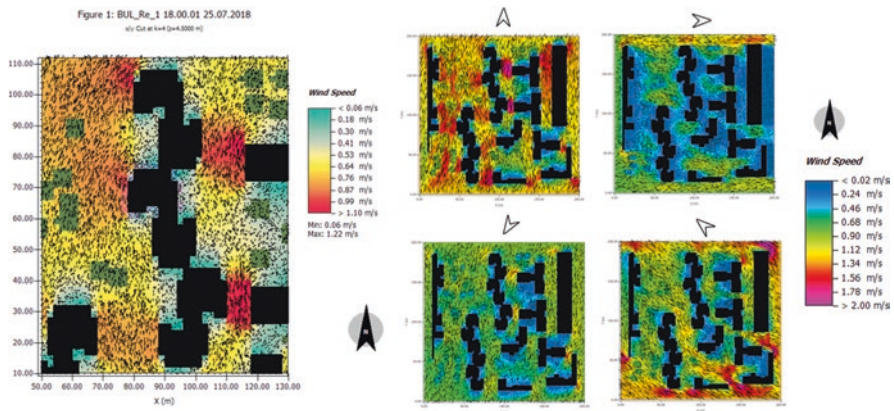


Fig. 5.23 ENVI-met results of the airflow at 4.5 m above ground level around the case study building for different dominant wind directions

wind pressure at each opening in the EnergyPlus simulations. The results showed significant reduction of the ventilation rates in some of the rooms (up to  $-35\%$  in comparison to the standard pressure coefficient approach). In summer, the reduction of the ventilation rates has a clear negative impact on indoor thermal comfort, increasing the operative temperatures and overheating hours. The maximum increase of the indoor operative temperature due to reduced ventilation rates reached  $3.7\text{ }^{\circ}\text{C}$  at night, when the outdoor temperature decreased, and the natural ventilation had the maximum cooling potential. Larger discrepancies in the building ventilation rates were found for higher meteorological wind speeds.

These results confirm that the selection of a suitable weather file and microclimatic conditions is essential for more accurate predictions of internal thermal comfort and will assist in the sizing of passive and active systems to avoid overheating.

## 5.5 Chapter Summary

This chapter gave an outline of urban microclimate characteristics focusing on locations in high latitudes and its impact on comfort and energy demand. Throughout the chapter, London has been used as an example of a high-latitude location; results from various studies in London over the last two decades are presented including recent studies of urban albedo.

The relationship of surface and air UHI in high-latitude cities was described based on available literature at global scale. Energy demand is mostly affected by microclimatic air temperature while comfort is also affected by radiant temperature and wind patterns. In London, the average annual UHI is  $2.5\text{ }^{\circ}\text{C}$  at night but there is wide variation including cool islands mainly during the day. It was found that night UHI is independent of daytime air temperature during the summer; during the night similar difference between urban and rural air temperature was measured during a typical and hot week. A computational study was carried out on the impact of UHI using current and future weather files on energy demand and overheating for office buildings. As expected, energy demand for cooling is higher within the UHI. It was shown that offices with medium internal heat gains without night free cooling have similar cooling demand to offices with high heat gains and night free cooling. In the future, and because of higher night temperature due to the combined effect of climate change and UHI, offices with medium internal heat gains perform better than those with night free cooling. The study also concluded that as expected heating demand is lower in offices within the UHI and even lower in the future. Mitigation strategies are outlined with the suggestion that improving the external thermal environment is the main outstanding issue where further research is needed.

Of the parameters affecting external thermal environment vegetation and surface albedo have potentially a pronounced impact on the microclimate and were explored further. Measurements in London have shown that air temperatures are lower within the UHI in areas with vegetation. The effect of surface albedo was also measured indicating that reflective surfaces on the ground and on roofs can improve local

microclimate by reducing surface temperatures. The effect of building facade albedo was studied in central London showing that dark-coloured facades result in higher surface temperatures, but overshadowing effects were clear.

Studies of urban albedo indicate that the contribution can be grouped into five interrelated parameters: (a) geometry—the geometry of individual buildings, the building group geometry and the geometry of buildings in relation to roads, usually referred to as urban canyon geometry; (b) reflectance of surfaces and their orientation—ground, facades and roofs; (c) sun altitude and azimuth determining the incidence angle of incoming solar radiation with strong seasonal contrasts in high latitudes; (d) moisture of permeable surfaces (soil) and altering reflectivity of impermeable surfaces; and (e) vegetation acting as obstruction to the incoming radiation and reflection paths. Of these (a) and (b) are not related to climate and latitude while (c), (d) and (e) are closely related to climate. Models have been developed to predict urban albedo mainly based on computational analysis with the aim to predict the impact on energy demand by buildings which have developed indices for these parameters such as the canyon aspect ratio which affects the amount of solar radiation incident on the canyon surfaces, building density which is the ratio of the buildings' footprint area to the urban site area and ratio of the vertical surface area that defines the facade density. Results of measurements and computational analysis for an area in London and their impact on urban albedo have been presented.

Approaches to include local microclimate in the energy performance simulations of buildings in urban contexts have been presented in Sect. 5.4 based on the use of a suite of climate tools such as Urban Weather Generator, calculation of the canyon wind speed by applying different empirical models and ENVI-met which allows to simulate the spatial and temporal distribution of the airflow around buildings, considering the actual three-dimensional geometry of the building and its surroundings. A case study in London was presented as an example of the potential impact of the microscale airflow on the indoor thermal conditions of buildings. The results showed significant reduction of the ventilation rates in some of the internal spaces resulting in a clear negative impact on indoor thermal comfort, increasing the operative temperatures and overheating hours.

**Acknowledgement** This work was funded by EPSRC, UK, under the project 'Urban albedo computation in high latitude locations: An experimental approach' (EP/P02517X/1).

## References

- Akbari, H., & Kolokotsa, D. (2016). Three decades of urban heat islands and mitigation technologies research. *Energy and Buildings*, 133, 834–842.
- Alchapar, N. L., & Correa, E. N. (2016). The use of reflective materials as a strategy for urban cooling in an arid "OASIS" city. *Sustainable Cities and Society*, 27, 1–14. <https://doi.org/10.1016/j.scs.2016.08.015>.



- Bueno, B., Norford, L., Hidalgo, J., & Pigeon, G. (2013). The urban weather generator. *Journal of Building Performance Simulation*, 6(4), 269–281. <https://doi.org/10.1080/19401493.2012.718797>.
- Chen, D., & Weiteng, H. (2013). Using the Köppen classification to quantify climate variation and change: An example for 1901–2010. *Environmental Development*, 6, 69–79. <https://doi.org/10.1016/j.envdev.2013.03.007>].
- Erell, E., Pearlmutter, D., Boneh, D., & Kutiel, P. B. (2014). Effect of high-albedo materials on pedestrian heat stress in urban street canyons. *Urban Climate*, 10, 367–386.
- Ghiaus, C., Allard, F., Georgiakakis, C., Santamouris, M., Roulet, C.-A., Germano, M., & Tilenkamp, F. (2004). URBVENT WP1 final report: Soft computing of natural ventilation potential. In *URBVENT: Natural ventilation in urban areas-potential assessment and optimal façade design. European commission*. London: Routledge. <https://doi.org/10.4324/9781849772068>.
- Hoppe, P. (1999). The physiological equivalent temperature—A universal index for the biometeorological assessment of the thermal environment. *International Journal of Biometeorology*, 43, 71–75.
- Huttner, S., & Bruse, M. (2009). Numerical modeling of the urban climate—A preview on ENVI-MET 4.0, in *The seventh International Conference on Urban Climate. Yokohama, Japan*. Retrieved from [http://www.ide.titech.ac.jp/~icuc7/extended\\_abstracts/pdf/382880-2-090514010851-002.pdf](http://www.ide.titech.ac.jp/~icuc7/extended_abstracts/pdf/382880-2-090514010851-002.pdf).
- Kolokotroni, M., & Giridharan, R. (2008). Urban Heat Island Intensity in London: An investigation of the impact of physical characteristics on changes in outdoor air temperature during summer. *Solar Energy*, 82, 986–998.
- Kolokotroni, M., Giannitsaris, I., & Watkins, R. (2006). The effect of the London Urban Heat Island on building summer cooling demand and night ventilation strategies. *Solar Energy*, 80(4), 383–392.
- Kolokotroni, M., Ren, X., Davies, M., & Mavrogianni, A. (2012). London’s urban heat island: Impact on current and future energy consumption for heating and cooling. *Energy and Buildings*, 47, 302–311.
- Kolokotroni, M., Gowreesunder, B., & Giridharan, R. (2013). Cool roof technology in London: An experimental and modelling study. *Energy and Buildings*, 67, 658–667. <https://doi.org/10.1016/j.enbuild.2011.07.011>.
- Levinson, R. (2019). Using solar availability factors to adjust cool-wall energy savings for shading and reflection by neighboring buildings. *Solar Energy*, 180, 717–734. <https://doi.org/10.1016/j.solener.2019.01.023>.
- Maciel, C. R., & Kolokotroni, M. (2017). Cool materials in the urban built environment to mitigate heat islands: Potential consequences for building ventilation. *38th AIVC International Conference, 13–14 Sep 2017, Nottingham, UK*.
- Maciel, C. R., Kolokotroni, M., Nogueira, M. C. J. A., Giridharan, R., & Watkins, R. (2013). The impact of surface characteristics on ambient temperature at urban micro-scale: Comparative field study in two climates. *International Journal of Low Carbon Technologies*. <https://doi.org/10.1093/ijlct/ctt016>.
- Mao, J., Yang, J. H., Afshari, A., & Norford, L. K. (2017). Global sensitivity analysis of an urban microclimate system under uncertainty: Design and case study. *Building and Environment*, 124, 153–170. <https://doi.org/10.1016/j.buildenv.2017.08.011>.
- Nikolopoulou, M., et al. (2020). Developing an Urban Albedo Calculator for London: The experimental campaign supporting the development of the tool. *CIBSE Technical Symposium, September 2020*.
- Pawlak, W., & Fortuniak, K. (2003). Application of the physical model to study effective albedo of the urban canyon, in: *Fifth International Conference on Urban Climate, Lodz, Poland*.
- Peng, S., Piao, S., Ciaisi, P., Friedlingstein, P., Otle, C., Breon, F. M., Nan, H., Zhou, L., & Myneni, R. B. (2012). Surface urban heat island across 419 global big cities. *Environmental Science & Technology*, 46(2), 696–703.

- Qin, Y. (2015). Urban canyon albedo and its implication on the use of reflective cool pavements. *Energy and Buildings*, 96, 86–94.
- ReCO2ST. (2020). *Residential Retrofit assessment platform and demonstrations for near zero energy and CO<sub>2</sub> emissions with optimum cost, health, comfort and environmental quality*. <https://reco2st.eu/>
- Salvati, A., & Kolokotroni, M. (2019). Microclimate data for building energy modelling: Study on ENVI-Met forcing data. In V. Corrado, E. Fabrizio, A. Gasparella, & F. Patuzzi (Eds.), *Proceedings of the 16th IBPSA Conference 2019, 2–4 September 2019, Rome, Italy* (pp. 3361–3368). Rome: IBPSA. <https://doi.org/10.26868/25222708.2019.210544>.
- Salvati, A., & Kolokotroni, M. (2020a). Impact of urban albedo on microclimate and thermal comfort over a heat wave event in London. In S. Roaf, F. Nicol, & W. Finlayson (Eds.), *WINDSOR 2020: Resilient Comfort. Proceedings. Cumberland Lodge, 16–19 April 2020, Windsor UK* (pp. 566–578). London: WINDSOR.
- Salvati, A. and Kolokotroni, M. (2020b). Impact of urban albedo on microclimate: Computational investigation in London. *35th PLEA Conference, sustainable architecture and urban design, planning post carbon cities, A Coruna, Spain, 1–3 September 2020*.
- Salvati, A., Palme, M., Chiesa, G., & Kolokotroni, M. (2020). Built form, urban climate and building energy modelling: Case-studies in Rome and Antofagasta. *Journal of Building Performance Simulation*, 13, 209–225. <https://doi.org/10.1080/19401493.2019.1707876>.
- Santamouris, M. (2007). Heat Island Research in Europe: The state of the art. *Advances in Building Energy Research*, 1(1), 123–150. <https://doi.org/10.1080/17512549.2007.9687272>.
- Santamouris, M. (2015). Analyzing the heat island magnitude and characteristics in one hundred Asian and Australian cities and regions. *Science of the Total Environment*, 512–513, 582–598.
- Santamouris, M. (2016). Innovating to zero the building sector in Europe: Minimising the energy consumption, eradication of the energy poverty and mitigating the local climate change. *Solar Energy*, 128, 61–94.
- Santamouris, M. (2020). Recent progress on urban overheating and heat island research. Integrated assessment of the energy, environmental, vulnerability and health impact. Synergies with the global climate change. *Energy and Buildings*, 207, 109482.
- Urban Albedo Project. (2019). <https://research.kent.ac.uk/urbanalbedo/>.
- Watkins, R., Palmer, J., Kolokotroni, M., & Littlefair, P. (2002a). The London Heat Island—Results from summertime monitoring. Proc. Chartered Institution of Building Services Engineers, Series A. *Building Services Engineering Research and Technology*, 23(2), 97–106.
- Watkins, R., Palmer, J., Kolokotroni, M., & Littlefair, P. (2002b). The London Heat Island—Surface and air temperature measurements in summer 2000. *ASHRAE Transactions*, 108(Pt1), 419–427.
- World Atlas. (2020). *Köppen climate classification system*. <https://www.worldatlas.com/articles/what-is-the-koppen-climate-classification-system.html>.
- Xu, X., Azari Jafari, H., Gregory, J., Norford, L., & Kirchain, E. (2020). An integrated model for quantifying the impacts of pavement albedo and urban morphology on building energy demand. *Energy and Buildings*, 211, 109759.
- Yang, X., & Li, Y. (2015). The impact of building density and building height heterogeneity on average urban albedo and street surface temperature. *Building and Environment*, 90, 146–156.
- Zhou, D., Zhao, S., Liu, S., Zhang, L., & Zhu, C. (2014). Surface urban heat island in China's 32 major cities: Spatial patterns and drivers. *Remote Sensing of Environment*, 152, 51–61.